

Setup of an Electric Car Charging Device with a PV Grid

Vishnuvardhan Vadla

Electrical and Electronics Engineering, St. Martin's Engineering College

vishnuvardhaneee@smec.ac.in

Abstract- This paper introduces an experimental approach on control Electric Photovoltaic Vehicle Charging System (PV) Array, converters, emulator power grid and programmable DC Electronic charging reflecting an emulator of the Li-ion battery. The Conceived device will supply the battery simultaneously with PV Power generation. The goal of the applied control approach is to extract Max PV array control and the man. The experimental experiment Results obtained with controller board dSPACE 1103, display The system reacts within certain limits and confirms the system and the Such system's importance to electric vehicle charging.

Keywords- renewable energy integration, photovoltaic, battery electric vehicles, public grid, control charging system.

I. INTRODUCTION

Improved quality of life and greater mobility contribute to improved higher energy consumption, and suggested Gas emissions from green houses. The increased electricity consumption implies greater efficiency and reliability in electricity control Flows, less mismatching between the production of electricity and Request, and renewable energy more incorporated. So, the in recent years the idea of a smart grid has been born. A Clever Grid Can easily be described as the supply of electricity, Transporting, transforming and effectively distributing electricity (From suppliers to consumers), included in the Information Technology and Communications. The principal aim is to better balance power generation and smart grid with cameras, communications and power consumption Technology Tracking. The smart grid will then be used as a package shaped by three-layer interaction: power transportation and layer of distribution, communication and sensors, and Applications and resources layer of applications.

Considering the electric needs of tomorrow, such as electric vehicles balancing the demand of power and the output of electricity is to boost the reliability of the grid while decreasing the Amount of power outages is an immense problem indeed. Currently, Plug-in hybrid electric cars and electric vehicles are a significant step in resolving environmental issues and are being installed across the globe. Multitudes Studies continue to maximize the performance of engines and batteries both for discharge and reload operations. This, however, is It is important to understand the further effects of PHEVs and Mostly recharging EVs on the electrical grid [1] [2]. Depending on when the vehicles are plugged in and where,

They could trigger severe grid constraints. THE

It is hoped the grid will not be significantly affected since the recharge will often take place during the night Uh, hours. The end-users however tend to plug in when Instead of using the electricity grid, it might be convenient for them, be solid. Be better. Renewable and distributed power, on the other hand, the share of the energy mix is rising, and its incorporation into the grid More than ever, an energy management system is connected to require. Therefore, one solution, from an environmental approach Condition is that all or part of the PHEVs and EVs are Paid from sources of renewable

energy [3] [4] [5]. It is difficult today to give between recharges an average of typical autonomy for EVs. Several manufacturers have announced a range of several tens of km of autonomy for soon-to-be EVs. Given the high mobility that exists today, it is probable that an EV driver would need to recharge the vehicle to operate throughout his stay, hence the opportunity to recharge with photovoltaic (PV) energy throughout daytime. There is a favorable political and economic background in urban areas, leading to a substantial growth of small PV power plants, thus connected to or incorporated into tertiary or residential buildings and car parks. Green Today the energy purchasing conditions lead these applications very naturally to a grid-connected system with complete and permanent injection of energy. However, given the technological constraints of the lack of a smart grid that can incorporate energy management, this creation may be The power back grid capability will be restrained. Ideally, at the moment it is produced electricity must be consumed, particularly true with peak demand, with minimal electrical losses along the power lines from power generation to end user. In this sense, the device that allows the EVs to charge directly from the PV power and a bidirectional energy flow from / to the grid is an alternative solution to those technical difficulties for houses, car parking and charging stations fitted with PV power plant. This system is a local generator of PV electricity, the priority of which is the generation of energy for self-feeding, with a grid link for further supply in the event of need and for the selling of excess energy. Via a smart meter the grid connection of this device must take into account the electrical grid's availability, needs and vulnerability. For control and billing purposes, a smart meter is able to relay information through a certain network back to the public grid.

This paper focuses on the PV grid-connected device control strategy, which enables a battery-powered electric vehicle (BEV) to be fed simultaneously and in the same position as the output of PV electricity. First, the device is described as several subsystems: photovoltaic array, power grid emulation and programmable electronic DC load, which imposes currents to simulate a Li-ion BEV operation. The purpose of the system control is to extract maximum power from the PV array and manage the transfer of power through the battery load, in terms of its charging status (SOC) and taking into account the availability and needs of the public grid. In order to pass the full PV power available at all times to the BEV, a technique for full power point tracking (MPPT) is implemented. The MPPT algorithm is Incremental Conductance [6][7] and aims to find the current reference for which PV will offer the maximum of its power in real time. A voltage control is implemented in accordance with an acceptable SOC in order to better simulate the Li-ion BEV charging. The test results obtained with a dSPACE 1103 controller board show that the device reacts within certain limits and confirms the validity of such configuration for the charging system of EVs.

II. CHARGING SYSTEM OF ELECTRIC VEHICLE

.Many small PV systems run in a grid-Connected mode, which does not require any local load interaction. The proposed system allows for both BEV connections as load, and public grid connections.

A. System Overview

The charging system for EVs with a grid-connected PV configuration is shown in Fig. 1. It is a matter of photovoltaic local power generation with an integrated energy management system that operates under the premise that where, when, and how it is generated is used. The public grid is only used as a backup and, if available. By self-feeding, this will remove energy demand from the electric grid and sell the surplus electricity only if the public grid requires it. Therefore the produced electricity must be consumed in the form of production for more energy efficiency; this is why we take into account the construction of charging points for BEVs. The public grid also provides the DC load when the sunlight is too poor to produce all the required power to pass to the BEVs. On the other hand, if the produced PV power is more important than the power needed by the BEVs, the device sends power back to the grid. The bidirectional flow of electricity from / to the grid is managed with the availability and needs of the public grid in mind. For this reason, in our university, an experimental platform and a test bench have been mounted, the images of which are given in Fig. 2. It mainly refers to 16 photovoltaic panels (2kWp, Fig. 2(a)), a weather station, a public grid simulator (linear 3kVA amplifier), a dSPACE 1103 controller board and necessary power electronics. This device is connected to a programmable electronic DC load (Chroma 63202, 2.6kW 500V-50A) that enables the standard BEV charge period to be simulated, Fig. (b) 2(b).

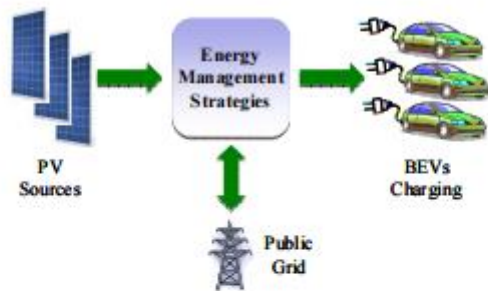


Figure 1. EVs charging station with PV grid-connected system.



Figure 2. (a) Image of PV array, (b) test bench.

B. PV Array Configuration

The PV array (PVA) consists of 16 Solar Fabric SF-130/2-125 PV panels, and its electrical specifications are shown in Table I. The electrical coupling is shown on the Fig. 3. There are two serial collections of four parallel divisions consisting of two PV panels in sequence.

To protect the PV panels against run-back current one diode D is put in each branch's head. RLIG symbolizes the resistance line, which reflects power line losses.

TABLE I ELECTRICAL STC SPECIFICATIONS OF PV PANEL

Solar-Fabrik SF-130/2-125	
N_s number of cells in series	36
I_{sc} short-circuit current	7.84A
V_{oc} open-circuit voltage	21.53V
I_{MPP} maximum power point current	7.14A
V_{MPP} maximum power point voltage	17.50V
K_0 temperature coefficient for current	0.00545A/K
θ^* temperature reference	298K
g^* solar irradiance reference	1000W/m ²

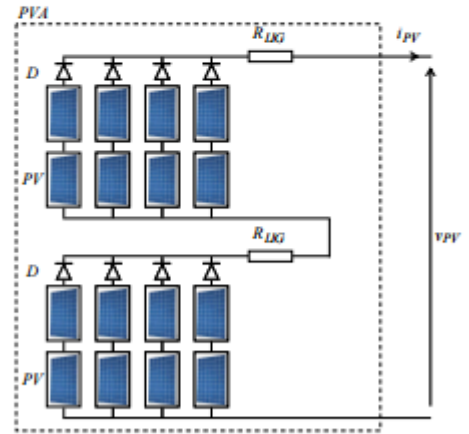


Figure 3. PV panels electrical coupling

C. Electrical system description

The BEV charging device, shown on Fig. 4, consists of 4-leg power converter (B1 to B4), previously mentioned PVA, BEV emulator, public grid (PG) emulator and a series of inductors and condensers to ensure compatibility between the various components. The system being studied is split into many subsystems.

$$\frac{di_{PV}}{dt} = \frac{1}{L_{PV}}(v_{PV} - v'_{PV})$$

$$\begin{bmatrix} i'_{PV} \\ v'_{PV} \end{bmatrix} = a_{PV} \begin{bmatrix} i_{PV} \\ v \end{bmatrix} \tag{1}$$

$$a_{PV} = \frac{1}{T} \int_0^T f_{B1} dt, a_{PV} \in [0;1]$$

1) PVA and impedance adapter subsystem

Via the B1 power converter leg and the LPV inductance, PVA is electrically coupled to the DC bus. Equations (1) model the PVA and Impedance Subsystem described as:

$$\underline{\underline{di_{PV}}} \approx \underline{\underline{\Delta i_{PV}}} = i_{PV}(z) - i_{PV}(z-1)$$

$$\underline{\underline{dv_{PV}}} \approx \underline{\underline{\Delta v_{PV}}} = v_{PV}(z) - v_{PV}(z-1) \tag{2}$$

PVA power depends on solar irradiance (g), PV cell temperature (θ), array voltage (vPV) and PVA (iPV) current.

The operating point of a PV generator-connected load does not always correspond with the optimum point and varies depending on the weather. To maximize the energy generated from the PVA, it is proposed to find and maintain the peak power using the Incremental Conductance (INC) MPPT process.

The INC MPPT algorithm uses the PV device conductivity derivative to evaluate the location of the operating point in relation to the maximum power point (MPP).

This procedure is conducted in this work in order to enforce the current reference i_{PV}^* . It is based, as in [8], on the fact that the

slope tangent of the characteristic $pPV - iPV$ ($pPV = vPV - iPV$) is zero in MPP, positive on the left side of MPP, and negative on the right side of MPP.

the derivate of the PVA impedance $PVPV = \frac{dv}{di}$

is used.

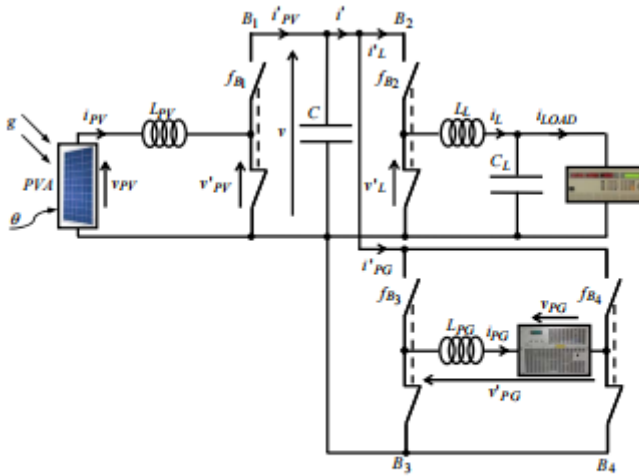


Figure 4. BEV charging electrical scheme.

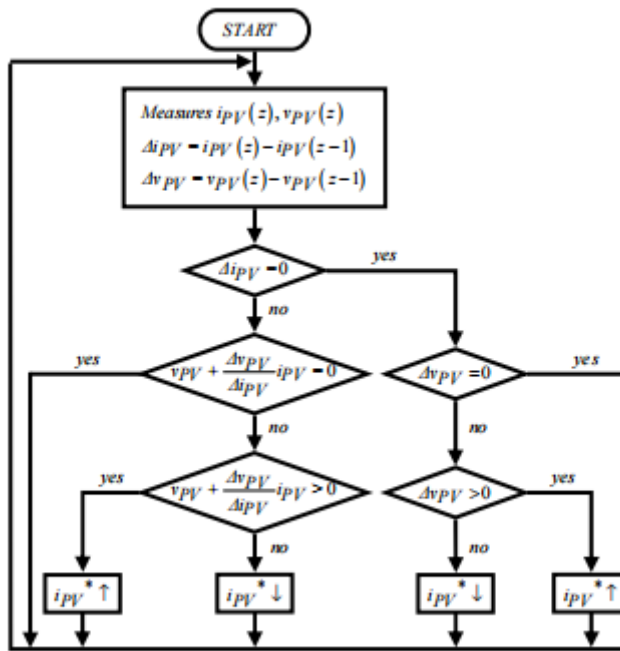


Figure 5. Flow chart of the INC algorithm.

2) DC Bus subsystem

The DC bus is composed of a C capacitor and a v voltage electrical coupling. The DC bus equations that run are:

$$\frac{dv}{dt} = \frac{1}{C}(i'_{PV} - i')$$

$$i' = i'_{PG} + i'_L$$

(3)

3) Battery Electric Vehicle Emulator subsystem

It is believed that the Li-ion battery is charged through a so-called CC / CV procedure [9]. This one involves charging a Li-ion battery in two modes, a mode of constant current (CC) followed by a mode of constant voltage (CV). The charge current remains constant

during CC mode until the voltage increases to a cut-off voltage. This voltage is 3.6V per cell in our case. It is believed that a battery control system balances all of the cells of the battery pack. The voltage remains constant throughout the CV mode, while the current decreases. A CC / CV procedure was applied to and reported on an A123 Li-Fe PO4 26650 cell. A CC / CV profile proportional to the profile reported on one cell shall be considered to emulate the BEV charge.

By imposing the current into the load (i_{LOAD}) and regulating the voltage around the capacitor (v_{LOAD}), the Li-ion battery is emulated. For a standard charging period, the action of a Li-ion battery pack is emulated by a programmable electronic DC charge. By coupling 100 cells into series, the BEV current reference i^*_{LOAD} (Fig. 6) and BEV voltage reference v^*_{LOAD} (Fig. 7) are obtained.

Fig. Fig. 6 Displays a contrast between i^*_{LOAD} and i_{LOAD} , the evolutions of which are similar, except for the end of charging corresponding to the programmable DC electronic load behavior for low current value. With respect to the voltage evolution, both the reference voltage v^*_{LOAD} and the load voltage v_{LOAD} are the same as shown in Fig. 7.

The BEV emulator is wired electrically to the DC bus via the leg of the B2 power converter, LL inductance, and CL condenser. The equations for modeling are given by (4).

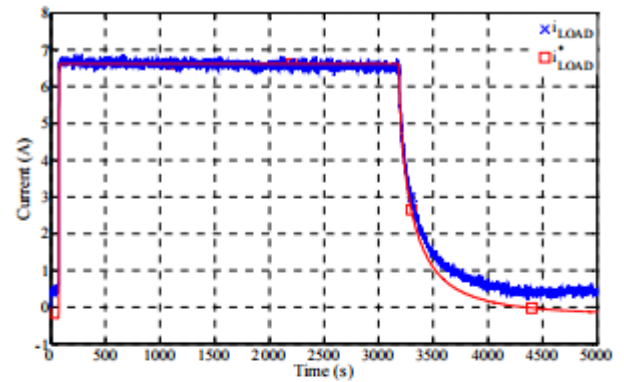


Figure 6. BEV current mode charge.

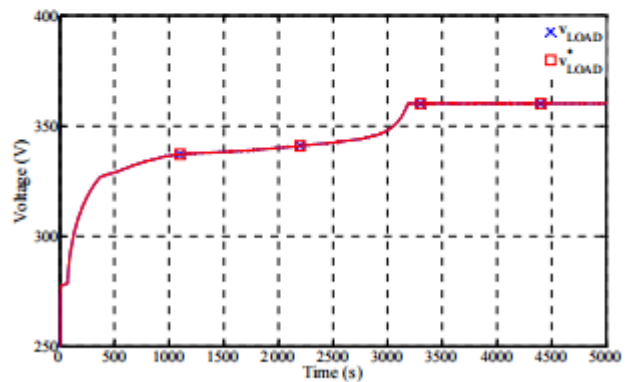


Figure 7. BEV voltage mode charge.

$$\begin{aligned} \frac{di_L}{dt} &= \frac{1}{L_L}(v'_L - v_{LOAD}) \\ \frac{dv_{LOAD}}{dt} &= \frac{1}{C_L}(i_L - i_{LOAD}) \\ \begin{bmatrix} i'_L \\ v'_L \end{bmatrix} &= a_L \begin{bmatrix} i_L \\ v \end{bmatrix} \\ a_L &= \frac{1}{T} \int_0^T f_{B2} dt, \quad a_L \in [0;1] \end{aligned} \quad (4)$$

4) Public Grid Emulator subsystem

Via the B3 and B4 power converter legs and the LPG inductance, the PG is electrically coupled to the DC bus. For bidirectional energy flow this connection is important. Thanks to that subsystem, the DC bus voltage v is protected. The equations for operation are given by (5).

$$\begin{aligned} \frac{di_{PG}}{dt} &= \frac{1}{L_{PG}}(v'_{PG} - v_{PG}) \\ \begin{bmatrix} i'_{PG} \\ v'_{PG} \end{bmatrix} &= a_{PG} \begin{bmatrix} i_{PG} \\ v_{PG} \end{bmatrix} \\ a_{PG} &= \frac{1}{T} \int_0^T (f_{B3} - f_{B4}) dt \quad \text{with } f_{B3} = \overline{f_{B4}} \\ a_{PG} &\in [-1;1] \end{aligned}$$

III. CONTROL SYSTEMS STRATEGY

The goal of the system control strategy is to extract maximum power from PVA and manage the transfer of power through the BEV with respect to its SOC.

Five state variables (i_{PV} , v , i_L , v_{LOAD} , and i_{PG}) are dominated by three settings (a_{PV}^* , a_L^* , and a_{PG}^*). The concepts of direct and indirect inversion are used to control this system: direct inversion (without controller) for items that are not time functions, indirect reversal (with controller) for items that are time functions.

The present i_{PV}^* reference is obtained as per the INC MPPT strategy. The control adopted shall be carried out in accordance with the a_{PV}^* setting mentioned in (6):

$$a_{PV}^* = \frac{-C_{PV}(i_{PV}^* - i_{PV}) + v_{PV}}{v} \quad (6)$$

Since the voltage v_{PV} is very noisy experimentally, there is no feedback control to this voltage. Controller CPV is an integral proportional form.

A nested current loop with voltage loop is required according to the BEV emulator's CC / CV charging procedure mentioned earlier. This control leads to equations which follow:

$$\begin{aligned} a_L^* &= \frac{C_{LI}(i_L^* - i_L) + v_{LOAD}}{v} \quad \text{with} \\ i_L^* &= C_{LV}(v_{LOAD}^* - v_{LOAD}) + i_{LOAD} \end{aligned} \quad (7)$$

As voltage v_{LOAD} and current i_{LOAD} are experimentally compensated, Controller CLI and CLV are proportional. The nested current-voltage loops have to be correctly uncoupled using the bandwidths of CLI and CLV controllers to ensure the proper

operation of the system; the current internal loop bandwidth is much greater than the outer loop voltage.

The last setting is:

$$a_{PG}^* = \frac{C_{PGI}(i_{PG}^* - i_{PG}) + v_{PG}}{v} \quad (8)$$

Controller CPGI is integral in proportion as CPV. The protection system must be defined in order to define i_{PG}^* . In this case the DC bus voltage control achieves the protection method. So the current adjustment for the DC buses I^* is specified by:

$$i^{**} = -C_{PGV}(v^* - v) + i'_{PV} \quad (9)$$

Where CPGV is the same corrector like CPGI, with the same Setting.

From (3) and (9), the following expression is obtained:

$$i'_{PG} = -C_{PGV}(v^* - v) + i'_{PV} - i'_{L} \quad (10)$$

Experimentally the currents i'_{PV} and i'_{L} are very loud, and are not subject to feedback control. Thus, neglecting the overall losses of B3 and B4 power converter legs and losses of LPG inductors, (10) could be translated to (11):

$$i_{PG}^* = \frac{v}{v_{PG}}(-C_{PGV}(v^* - v) + i'_{PV} - i'_{L}) \quad (11)$$

In this study synthesis for correction is not realized for all controllers.

IV. EXPERIMENTAL RESULTS AND DISCUSSION

The goal of this research is to validate a systematic methodology rather than strictly numerical outcomes. For this reason we don't give the numerical values of the different components of the device being studied. All the automatic controls introduced, mentioned earlier, are working satisfactorily although the assumptions about losses have been made to simplify them.

In comparison to the reference SOC*, the SOC by CC / CV mode charging obtained from i^*_{LOAD} and v^*_{LOAD} is shown in Fig. 8. Evolution of both SOC and SOC* is similar, except for the end of the charge that corresponds to the programmable DC electronic load activity for low current values. It is considered that these results allow the simulation of the typical BEV charging cycle through the programmable DC electronic load to be approved for this comprehensive device approach.

The EV charging system's experimental results with PV grid-connected configuration are presented at Fig. 9 for the evolution of solar irradiance g on 10 March 2010, starting from 1:30 pm in Compiègne, France.

In the following expressions of power, the experimental test results are given: $p_{PV} = v_{PV} i_{PV}$ power provided by the PVA, $p_{LOAD} = v_{LOAD} i_{LOAD}$ power requested by the BEV and $p_{PG} = v_{PG} i_{PG}$ public grid transfer power. Fig. Fig. 9 indicates the evolution of solar irradiance g and of the EV charging system. Second, it is shown that the INC MPPT algorithm implemented works correctly in proportion to solar irradiance $p_{PV} g$.

We observe that the approach described earlier is well regarded for the time span considered. The public grid supplies electricity for $p_{PV} < p_{LOAD}$, it receives energy in comparison. Regarding the protection system, regardless of the sign and amplitude of the power difference between p_{PV} and p_{LOAD} , these results indicate that this experimental system is safe.

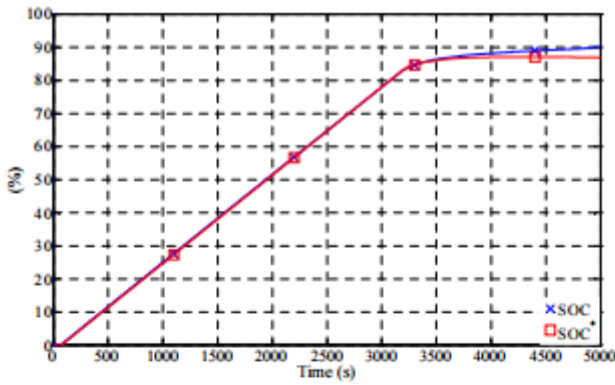


Figure 8. BEV SOC and reference SOC*.

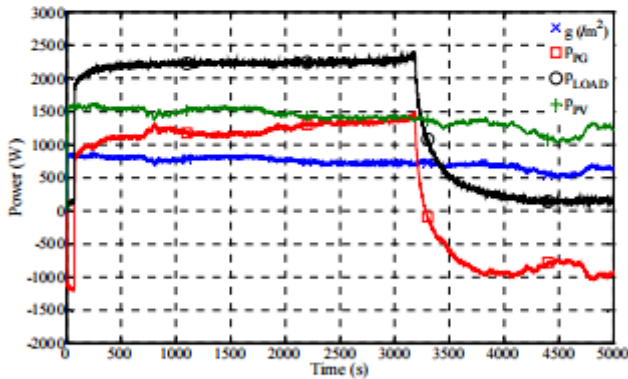


Figure 9. Solar irradiance g evolution on March 10th in 2010 starting from 30 pm at Compiègne and EV charging system powers evolutions (p applied by PV system versus g solar irradiance, p_{LOAD} absorbed by BEV, at p_{PG} for public grid).

Although the corrector needs adjustments to mitigate disruptions, the DC bus voltage remains at a constant value. On the other hand, machine losses are found by the balance of forces. These are not the focus of this research, but they must definitely be taken into account to boost the energy efficiency of the EV charging system.

In conclusion, it is observed that within the outlined plan, the overall framework, as planned, responds satisfactorily.

The availability, needs and insecurity of the electric grid should be taken into account with regard to the system's grid connection. Let us presume that a special smart device can receive information from the public grid through some network in the future and can also send back information.

Therefore, in order to better notify the device of public grid availability, the implementation of a KPG coefficient with $KPG \in \{0, 1\}$ in (11) could be a very simple procedure. Transform Equation (11) into (12):

$$i_{PG}^* = K_{PG} \cdot \frac{v}{v_{PG}} (-C_{PGV} (v^* - v) + i'_{PV} - i'_{L})$$

The EV charging device works as highlighted for public grid unlimited availability $KPG = 1$ and either $p_{PV} > p_{LOAD}$ or $p_{PV} < p_{LOAD}$.

For public grid unavailability $KPG = 0$ and $p_{PV} > p_{LOAD}$, the EV charging system operates under very restrictive condenser C-sizing conditions. In this case, some additional means of storage

must be inserted in the device. For $p_{PV} < p_{LOAD}$, the EV charging system's sine qua non operating requirement is to incorporate sources such as storage[10], micro-co generation unit (green coal, wood-pellets or sterling engines), or fuel cell. Also, regulation of accessibility limited by the public grid must be well planned. The problem of "single supply" or "single injection" may be more completely or partially supplied or injected, involving measured KPG values corresponding to public grid conditions and even unidirectional regulation of the legs of the B3 and B4 power converters. .

V. CONCLUSIONS

The Smart grid of optimized renewable energy affects both the utilities and end-users alike. In the next ten years, the smart grid might include house power "routers" at the residential level, whose purpose is to handle and supply every home appliance intelligently by minimizing and redirecting overall consumption. The primary objective of power providers could be the management of real-time demand in order to change their production of electricity, for end consumers it could be the real-time regulation of energy consumption, like the EV charging system. An experimental EV charging strategy was presented with PV grid-connected control of system. The device control strategy seeks to derive full power from the PV array and, with regard to its SOC, handle the energy flow through the BEV. The experimental results are obtained by numerical modeling implemented under MATLAB-Simulink and a controller board dSPACE 1103. A easy and swift control to enforce was done in this work. This control was not inherently designed to boost the BEV system's worldwide energy efficiency or life cycle. The goal for this first approach was to check the viability of the proposed control system.

The results show that the device can supply BEVs at the same time as the output of PV energy and that it reacts to PV power and public grid availability within certain limits. The test results obtained indicate that the proposed control can be used successfully for buildings and car parks fitted with a PV power plant.

Further study is to model the behavior of EV charging as an operating subsystem under the supervisory device as a control-command subsystem with a PV grid-connected framework. In order to achieve more efficient power transmission with minimized public grid effect, the approach chosen will take into account the uncertainties about PV power supply, public grid availability and BEV request.

REFERENCES

- [1]. S. D. Jenkins, J. R. Rossmairer, and M. Ferdowsi, "Utilization and effect, of plug-in hybrid electric vehicles in the United States power grid", in: *Proc. IEEE Vehicle Power and Propulsion Conference, VPPC 2008*.
- [2]. EPRI, "Environmental Assessment of Plug-In Hybrid Electric Vehicles; Volume 1: Nationwide Greenhouse Gas Emissions", Final Report, July 2007.
- [3]. V. Marano and G. Rizzoni, "Energy and Economic Evaluation of PHEVs and their Interaction with Renewable Energy Sources and the Power Grid", in: *Proc. IEEE International Conference on Vehicular Electronics and Safety, 2008*.
- [4]. Y. Gurkaynak and A. Khaligh, "Control and Power Management of a Grid Connected Residential Photovoltaic System with Plug-in Hybrid Electric Vehicle (PHEV) Load", in *Proc. IEEE Applied Power Electronics Conference and Exposition, APEC 2009*.
- [5]. X. Li, L. A. C. Lopes, and S. S. Williamson, "On the suitability of plug-in hybrid electric vehicle (PHEV) charging infrastructures based on wind and solar energy", in: *Proc. IEEE Power & Energy Society General Meeting, PES 2009*.
- [6]. V. Salas, E. Olias, A. Barrado, and A. Lazaro, "Review of the maximum power point tracking algorithms for stand-alone photovoltaic systems", *Solar Energy Materials and Solar Cells* 90-11, pp. 1555-1578, 2006.

- [7]. T. ESRAM and P. L. Chapman, "Comparison of photovoltaic array maximum power point tracking techniques", *IEEE Transactions on Energy Conversion* 22-2, pp. 439, 2007.
- [8]. I. Houssamo, F. Locment and M. Sechilariu. "Maximum power tracking for photovoltaic power system: Development and experimental comparison of two algorithms", *Renewable Energy* 35-10, pp. 2381- 2387, 2010.